Since January 2020 Elsevier has created a COVID-19 resource centre with free information in English and Mandarin on the novel coronavirus COVID-19. The COVID-19 resource centre is hosted on Elsevier Connect, the company's public news and information website.

Cell Reports

Report

Resistance of SARS-CoV-2 variants to neutralization by antibodies induced in convalescent patients with COVID-19

Graphical abstract

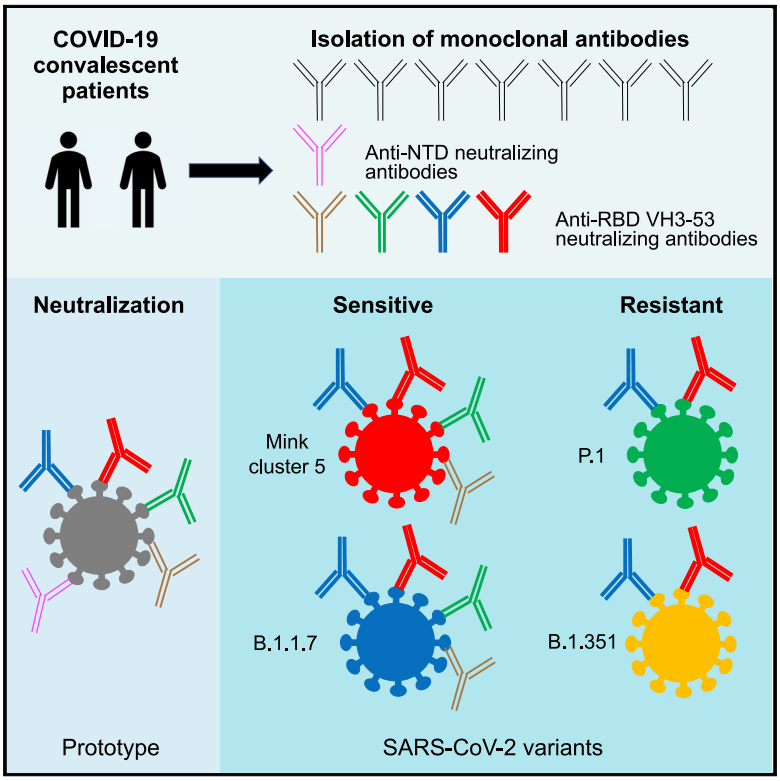

Highlights

- Neutralizing mAbs against SARS-CoV-2 are isolated from two convalescent patients
- Efficacy of antibodies is maintained against B.1.1.7 and mink cluster 5 variants
- B.1.351 from South Africa and P.1 from Brazil are resistant to mAbs and plasmas
- mAbs with high affinity for the RBD efficiently cross-neutralize B.1.351 and P.1

Authors

Yu Kaku, Takeo Kuwata, Hasan Md Zahid, ..., Yoshio Koyanagi, Hajime Iwagoe, Shuzo Matsushita

Correspondence

tkuwata@kumamoto-u.ac.jp (T.K.), shuzo@kumamoto-u.ac.jp (S.M.)

In brief

Kaku et al. demonstrate that the efficacy of neutralizing mAbs and convalescent plasma is maintained against SARS-CoV-2 variants B.1.1.7 from the UK and mink cluster 5 but decreases against B.1.351 from South Africa and P.1 from Brazil. Rapid spread of these variants significantly impacts SARS-CoV-2 therapies and vaccine strategies.

Kaku et al., 2021, Cell Reports *36*, 109385
July 13, 2021
https://doi.org/10.1016/j.celrep.2021.109385

CellPress

Cell Reports

CellPress
OPEN ACCESS

Report

Resistance of SARS-CoV-2 variants to neutralization by antibodies induced in convalescent patients with COVID-19

Yu Kaku,[1,15] Takeo Kuwata,[1,15,*] Hasan Md Zahid,[1] Takao Hashiguchi,[2,3] Takeshi Noda,[4,5] Noriko Kuramoto,[1] Shashwata Biswas,[1] Kaho Matsumoto,[1] Mikiko Shimizu,[1] Yoko Kawanami,[1] Kazuya Shimura,[6] Chiho Onishi,[6] Yukiko Muramoto,[4] Tateki Suzuki,[3] Jiei Sasaki,[3] Yoji Nagasaki,[7] Rumi Minami,[8] Chihiro Motozono,[9] Mako Toyoda,[9] Hiroshi Takahashi,[10] Hiroto Kishi,[10] Kazuhiko Fujii,[10] Tsuneyuki Tatsuke,[11] Terumasa Ikeda,[12] Yosuke Maeda,[13] Takamasa Ueno,[9] Yoshio Koyanagi,[6] Hajime Iwagoe,[14] and Shuzo Matsushita[1,16,*]

[1]Division of Clinical Retrovirology, Joint Research Center for Human Retrovirus infection, Kumamoto University, Kumamoto 860-0811, Japan
[2]Labolatory of Medical Virology, Institute for Frontier Life and Medical Sciences, Kyoto University, Kyoto 606-8507, Japan
[3]Department of Virology, Faculty of Medicine, Kyushu University, Fukuoka 812-8582, Japan
[4]Laboratory of Ultrastructural Virology, Institute for Frontier Life and Medical Sciences, Kyoto University, Kyoto 606-8507, Japan
[5]CREST, Japan Science and Technology Agency, Kawaguchi, Japan
[6]Laboratory of Systems Virology, Institute for Frontier Life and Medical Sciences, Kyoto University, Kyoto 606-8507, Japan
[7]Division of Infectious Diseases, Clinical Research Institute, National Hospitalization Organization, Kyushu Medical Center, Fukuoka, Japan
[8]Internal Medicine, Clinical Research Institute, National Hospital Organization, Kyushu Medical Center, Fukuoka, Japan
[9]Division of Infection and immunity, Joint Research Center for Human Retrovirus infection, Kumamoto University, Kumamoto 860-0811, Japan
[10]Department of Respiratory Medicine, Kumamoto City Hospital, Kumamoto 862-8505, Japan
[11]Faculty of Advanced Science and Technology, Kumamoto University, Kumamoto 860-8555, Japan
[12]Division of Molecular Virology and Genetics, Joint Research Center for Human Retrovirus Infection, Kumamoto University, Kumamoto 860-0811, Japan
[13]Department of Microbiology, Faculty of Life Sciences, Kumamoto University, Kumamoto 860-8556, Japan
[14]Department of Infectious Disease, Kumamoto City Hospital, Kumamoto 862-8505, Japan
[15]These authors contributed equally
[16]Lead contact
*Correspondence: tkuwata@kumamoto-u.ac.jp (T.K.), shuzo@kumamoto-u.ac.jp (S.M.)
https://doi.org/10.1016/j.celrep.2021.109385

SUMMARY

Administration of convalescent plasma or neutralizing monoclonal antibodies (mAbs) is a potent therapeutic option for coronavirus disease 2019 (COVID-19) caused by severe acute respiratory syndrome coronavirus 2 (SARS-CoV-2) infection. However, SARS-CoV-2 variants with mutations in the spike protein have emerged in many countries. To evaluate the efficacy of neutralizing antibodies induced in convalescent patients against emerging variants, we isolate anti-spike mAbs from two convalescent COVID-19 patients infected with prototypic SARS-CoV-2 by single-cell sorting of immunoglobulin-G-positive (IgG^+) memory B cells. Anti-spike antibody induction is robust in these patients, and five mAbs have potent neutralizing activities. The efficacy of most neutralizing mAbs and convalescent plasma samples is maintained against B.1.1.7 and mink cluster 5 variants but is significantly decreased against variants B.1.351 from South Africa and P.1 from Brazil. However, mAbs with a high affinity for the receptor-binding domain remain effective against these neutralization-resistant variants. Rapid spread of these variants significantly impacts antibody-based therapies and vaccine strategies against SARS-CoV-2.

INTRODUCTION

Severe acute respiratory syndrome coronavirus 2 (SARS-CoV-2) causes coronavirus disease 2019 (COVID-19), which emerged in late 2019 and became a pandemic (Wu et al., 2020a; Zhou et al., 2020; Zhu et al., 2020). A potent option to treat patients with COVID-19 is the administration of plasma from patients who have recovered from COVID-19 (Duan et al., 2020; Li et al., 2020; Liu et al., 2020b). Neutralization of viruses by antibodies is considered the main mechanism to control COVID-19 by convalescent plasma. Currently, hundreds of monoclonal antibodies (mAbs) against SARS-CoV-2 have been isolated from convalescent COVID-19 patients (Barnes et al., 2020; Brouwer et al., 2020; Cao et al., 2020; Kim et al., 2021; Kreye et al., 2020; Liu et al., 2020a), and potent neutralizing mAbs, which mostly target the receptor-binding domain (RBD) of the SARS-CoV-2 spike (S) protein, have been developed for clinical use (Schäfer et al., 2021; Weinreich et al., 2021).

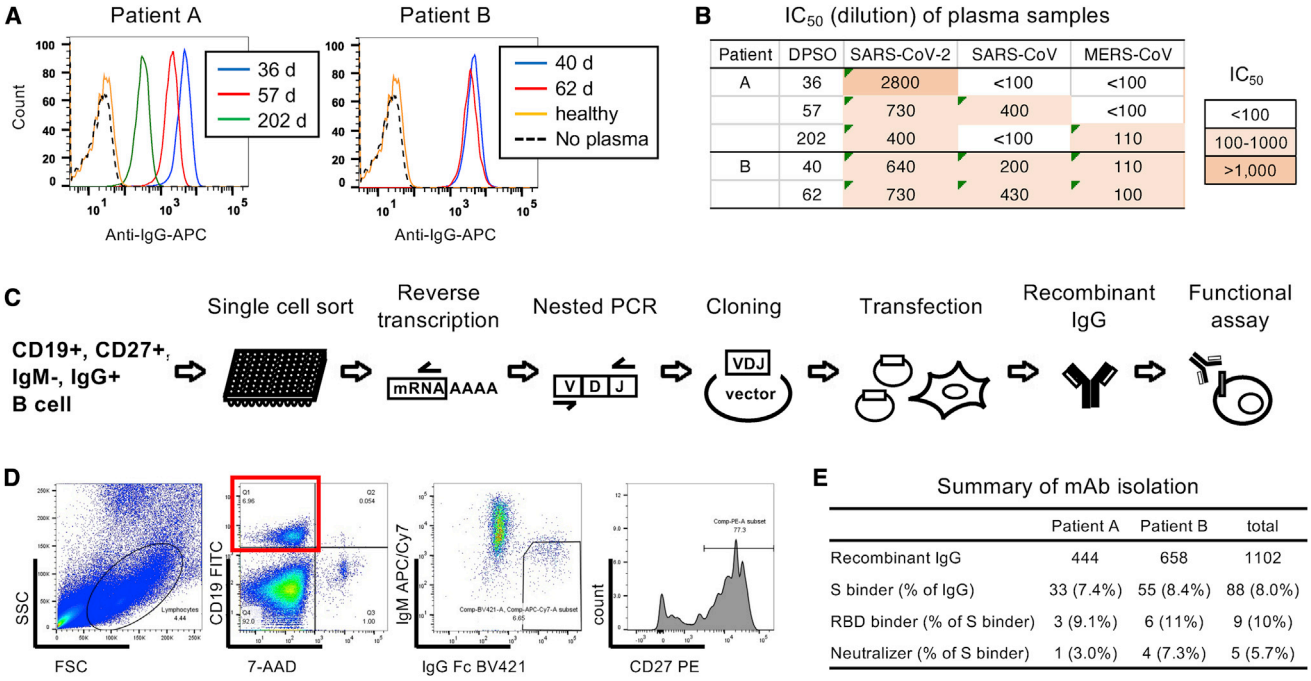

Figure 1. Isolation of neutralizing mAbs from two convalescent patients

(A) Binding activity of plasma samples from patients A and B to the SARS-CoV-2 S protein was analyzed by flow cytometry. Binding of IgG to cells expressing SARS-CoV-2 S at ×10,000 dilution of plasma samples is shown as a histogram. Dotted line, no plasma control; orange line, plasma from a healthy donor.

(B) Neutralization activity of plasma samples analyzed using pseudoviruses expressing the S protein from SARS-CoV-2, SARS-CoV, and MERS-CoV. IC_{50} values (dilution) are summarized.

(C) Strategy to isolate neutralizing mAbs is shown schematically.

(D) A representative flow cytometry plot is shown. $CD3^-CD14^-CD8^-$ cells were used to sort memory B cells ($7AAD^-CD19^+IgM^-IgG^+CD27^+$ cells), as shown in dotplots.

(E) Numbers of recombinant IgGs, S binders, RBD binders, and neutralizers from patients A and B are summarized.

New SARS-CoV-2 variants with multiple mutations in the S protein have emerged from the D614G variant (Elbe and Buckland-Merrett, 2017; Rambaut et al., 2020). Variants, including B.1.1.7 (also known as VOC-202012/01 or 501Y.V1) and B.1.351 (also known as 501Y.V2), have emerged in the UK and South Africa, respectively, and have since been detected in other countries (Leung et al., 2021; Tegally et al., 2021). P.1, In Brazil, a variant with unique mutations, has emerged in Brazil (Fujino et al., 2021; Maggi et al., 2021). It is important to clarify whether neutralizing antibodies from convalescent patients infected with the prototypic virus are effective against emerging SARS-CoV-2 variants for therapy using plasma or antibodies from convalescent patients. Therefore, we examined the sensitivity of neutralizing mAbs and plasma from convalescent patients to emerging SARS-CoV-2 variants.

RESULTS

Isolation of neutralizing mAbs from two convalescent patients

To identify potent neutralizing mAbs against SARS-CoV-2, we selected two patients, A and B, who had recovered from severe COVID-19 (Table S1). These patients were infected in March 2020, during the first wave of SARS-CoV-2 prevalence in Japan. Plasma samples from these patients had high binding activity to the SARS-CoV-2 Wuhan-Hu-1 S protein (Figures 1A and S1A). Significant binding of plasma samples to S was observed even at a 1:1,000,000 dilution, although the level of binding declined 202 days post-symptom onset (DPSO) in patient A. Neutralizing activity against SARS-CoV-2, which was measured using an HIV-1-based pseudovirus with the SARS-CoV-2 S protein carrying 614G, was detected in these plasma samples (Figure 1B). The potency of plasma sample neutralizing activity correlated with their binding activity, but their neutralizing activity, determined by 50% of the maximal inhibitory concentration (IC_{50}) values ranging from 1:640 to 1:2,800 dilution, was low compared with their strong binding activity (Figures 1A and S1A). Furthermore, these plasma samples had weak cross-neutralization activity against SARS-CoV and Middle East respiratory syndrome coronavirus (MERS-CoV) (Figure 1B).

We sorted IgG^+ memory B cells from patients A and B, and mAbs were produced from the amplified immunoglobulin genes (Figures 1C and 1D). The recombinant antibodies were screened for their reactivity to the S protein of SARS-CoV-2 Wuhan-Hu-1 strain (Figure 1E). S-binding antibodies were examined for their neutralizing activity using a pseudovirus expressing SARS-CoV-2 S. Overall, 444 and 658 antibodies were isolated from the immunoglobulin-G-positive (IgG^+) memory B cells of patients

CellPress
OPEN ACCESS

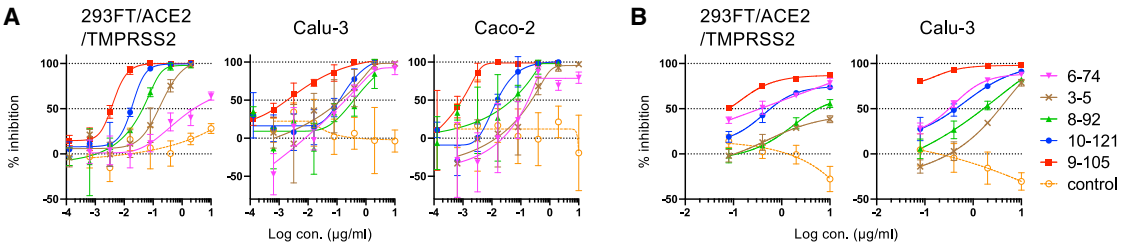

C

IC_{50} (μg/ml) of neutralizing mAbs isolated from convalescent patients

mAb	patient	SARS-CoV-2			SARS-CoV	MERS-CoV	Cell fusion	
		293FT/ACE2 /TMPRSS2	Calu-3	Caco-2	293FT/ACE2/TMPRSS2		293FT/ACE2 /TMPRSS2	Calu-3
6-74	B	2.6	0.20	0.18	>10	>10	0.36	0.32
3-5		0.16	0.14	0.24	>10	>10	>10	3.6
8-92		0.044	0.38	0.049	>10	>10	5.7	1.6
10-121		0.018	0.12	0.015	>10	>10	0.58	0.44
9-105	A	0.0035	0.0019	0.00092	>10	>10	<0.08	<0.08

IC_{50} (μg/ml)
>10
1-10
0.1-1
0.01-0.1
0.001-0.01
0.0001-0.001

D

Binding and genetic characteristics of neutralizing mAbs

mAb	Binding			H-chain		L-chain		CDRH3	
	RBD	NTD	KD (nM)	gene	SHM	gene	SHM	aa	length
6-74	-	+	ND	IGHV3-7	0	IGKV2-28	0.67	ARVHIHAPNYDILTGYYGTTPGYYYGMDV	29
3-5	+	ND	12.1	IGHV3-53	1.03	IGKV3-20	1.74	ARSYGDYFIDY	11
8-92	+	ND	0.576	IGHV3-53	2.05	IGKV1-9	1.77	ARDKNEGAMDV	11
10-121	+	ND	0.122	IGHV3-53	3.09	IGKV1-33	1.06	ARPIVGARAGMDV	13
9-105	+	ND	0.00203	IGHV3-53	2.05	IGKV3-20	2.44	ARDLEEAGGMDV	12

Figure 2. Characterization of five neutralizing mAbs

(A) Neutralization of SARS-CoV-2 pseudovirus by mAbs 6-74, 3-5, 8-92, 10-121, and 9-105 in 293FT/ACE2/TMPRSS2, Calu-3 (human lung cancer cell line), and Caco-2 (human colon adenocarcinoma cell line) cells is shown. A non-neutralizing mAb, 8-38, was used as a negative control (orange open circle).

(B) Cell fusion of 293FT/DSP8-11/SARS-CoV-2-S cells with 293FT/DSP1-7/ACE2/TMPRSS2 and Calu-3/DSP1-7 cells was measured by luciferase activity at 6 and 20 h after coculture, respectively. A non-neutralizing mAb, 5-76, was used as a negative control (orange open circle).

(C) IC_{50} values of the five mAbs are summarized.

(D) The binding and genetic characteristics of mAbs are summarized. Binding to RBD and NTD was analyzed by AlphaScreen. K_D values were determined by SPR analysis (Figure S1D). Gene usage (gene), somatic hypermutation % (SHM) of heavy and light chains, and CDRH3 amino acids (aa) and length were analyzed by IMGT vquest.

Data shown in (A) and (B) are represented as means ± SD (n = 3). See also Figure S1.

A and B, respectively (Figure 1E). Among the isolated antibodies, 33 (patient A, 7.4% of total antibodies) and 55 (patient B, 8.4% of total antibodies) were anti-S antibodies. One antibody (3.0% of anti-S antibodies) from patient A and four antibodies (7.3% of anti-S antibodies) from patient B neutralized SARS-CoV-2 pseudovirus (Figures 1E and 2).

Characterization of five neutralizing mAbs

Among the five neutralizing antibodies, 9-105, which was isolated from patient A 57 DPSO, potently neutralized SARS-CoV-2 pseudovirus at IC_{50} values of 3.5 ng/mL in 293FT/ACE2/TMPRSS2 cells, 1.9 ng/mL in Calu-3 cells, and 0.92 ng/mL in Caco-2 cells (Figures 2A and 2C). Analysis of their reactivity to RBD and the N-terminal domain (NTD) revealed that four neutralizing mAbs targeted the RBD and one targeted the NTD (Figure 2D). Four RBD-targeting neutralizing antibodies, including 9-105, used the *IGHV3-53* gene (Figure 2D), indicating that these mAbs were typical RBD-targeting neutralizing antibodies observed in patients with COVID-19 (Barnes et al., 2020; Brouwer et al., 2020; Cao et al., 2020; Gaebler et al., 2021; Kim et al., 2021; Kreye et al., 2020; Wu et al., 2020b). Similar to the mAbs previously reported, these mAbs had a low somatic hypermutation rate ranging from 1.03% to 3.09% in the *VH* gene and 1.06% to 2.44% in the *VK* gene (Figure 2D). One non-RBD-targeting antibody, 6-74, bound to the NTD of SARS-CoV-2 S protein and had an extremely long CDRH3 (Figure 2D). Neutralization activity of 6-74 was low compared with the RBD-targeting mAbs (Figures 2A and 2C), but it had a strong inhibitory activity against SARS-CoV-2 S-mediated cell fusion (Figures 2B and 2C). All the neutralizing mAbs specifically neutralized SARS-CoV-2 pseudovirus but did not cross-neutralize SARS-CoV or MERS-CoV pseudovirus in 293FT/ACE2/TMPRSS2 cells (Figure 2C). No neutralizing activity of mAbs against MERS-CoV was also confirmed by infection of pseudovirus to Caco-2 cells, which express a receptor for MERS-CoV, DPP4 (data not shown).

The neutralization potency of mAbs was proportional to their binding activity to the S protein on the cell surface, although the NTD-targeting mAb, 6-74, bound to the S protein with a greater affinity than the RBD-targeting mAbs with low neutralizing activity (Figure S1C). The binding activity of 6-74 was equivalent to 10-121, which had a 100-fold greater neutralizing activity against SARS-CoV-2 in 293FT/ACE2/TMPRSS2 compared with 6-74 (Figures 2C and S1C). The neutralizing activity of

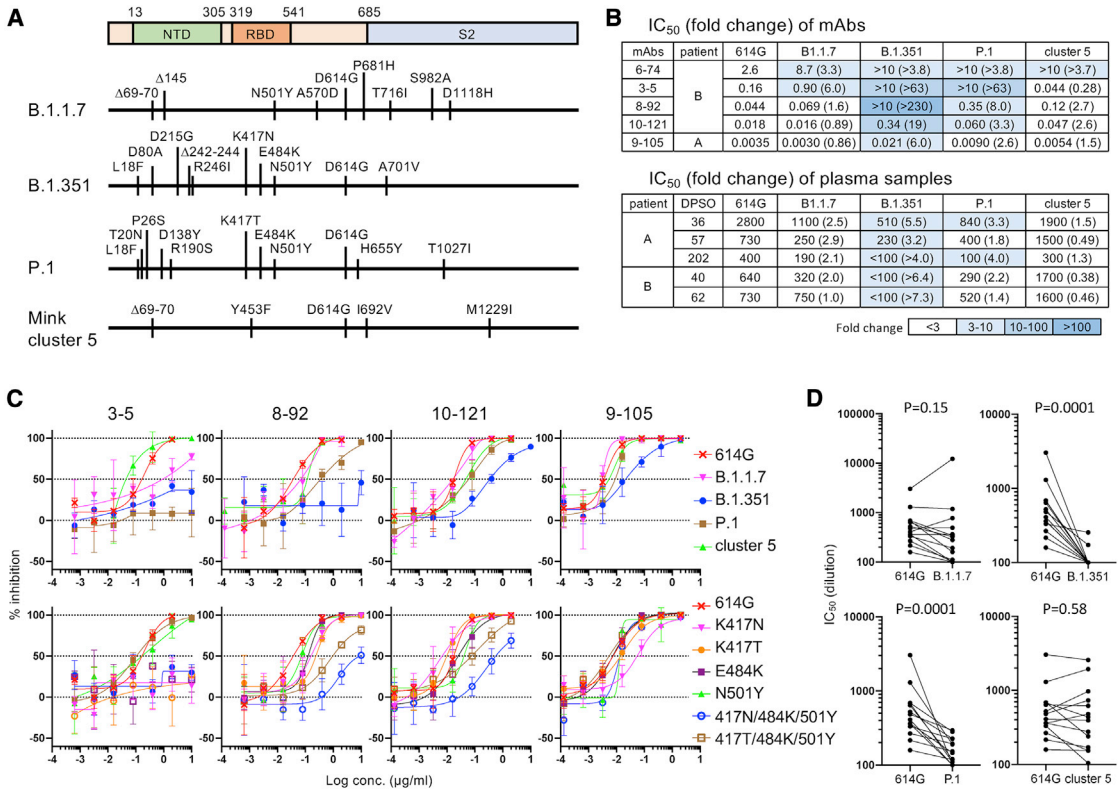

mAbs	patient	614G	B.1.1.7	B.1.351	P.1	cluster 5
6-74	B	2.6	8.7 (3.3)	>10 (>3.8)	>10 (>3.8)	>10 (>3.7)
3-5		0.16	0.90 (6.0)	>10 (>63)	>10 (>63)	0.044 (0.28)
8-92		0.044	0.069 (1.6)	>10 (>230)	0.35 (8.0)	0.12 (2.7)
10-121		0.018	0.016 (0.89)	0.34 (19)	0.060 (3.3)	0.047 (2.6)
9-105	A	0.0035	0.0030 (0.86)	0.021 (6.0)	0.0090 (2.6)	0.0054 (1.5)

patient	DPSO	614G	B.1.1.7	B.1.351	P.1	cluster 5
A	36	2800	1100 (2.5)	510 (5.5)	840 (3.3)	1900 (1.5)
	57	730	250 (2.9)	230 (3.2)	400 (1.8)	1500 (0.49)
	202	400	190 (2.1)	<100 (>4.0)	100 (4.0)	300 (1.3)
B	40	640	320 (2.0)	<100 (>6.4)	290 (2.2)	1700 (0.38)
	62	730	750 (1.0)	<100 (>7.3)	520 (1.4)	1600 (0.46)

Figure 3. Neutralizing activity against SARS-CoV-2 variants

(A) Amino acid substitutions in the S protein of SARS-CoV-2 variants B.1.1.7, B.1.351, P.1, and mink cluster 5 are schematically shown.

(B) IC_{50} values of mAbs (μg/mL) and plasma samples (dilution) against pseudoviruses with SARS-CoV-2 S variants are summarized with fold change (variant IC_{50} value/614G IC_{50} value).

(C) Neutralization of pseudoviruses with SARS-CoV-2 S variants (upper panels) and RBD mutants (lower panels) was examined by mAbs in 293FT/ACE2/TMPRSS2 cells. Data are represented as means ± SD (n = 3).

(D) IC_{50} values of plasma samples from 14 patients with COVID-19 other than patients A and B were compared between the 614G pseudovirus and pseudoviruses carrying the variant S protein. Statistical analysis was performed using a Wilcoxon matched-pairs signed rank test, and p values are shown.

RBD-targeting mAbs was also consistent with the results of surface plasmon resonance (SPR) analysis (Figure S1D). The most potent neutralizing mAb, 9-105, bound to RBD with a dissociation constant (K_D) of 2.03 × 10^{-12} M (Figures 2D and S1D). RBD-targeting mAbs with lower K_D values, indicating stronger binding activity, had higher neutralizing activity than RBD-targeting mAbs with higher K_D values.

Neutralization activity against SARS-CoV-2 variants

The neutralization potency of mAbs and plasma samples was examined against pseudoviruses expressing S proteins from the emerging SARS-CoV-2 variants, B.1.1.7 from the UK, B.1.351 from South Africa, P.1 from Brazil, and mink cluster 5 from Denmark (Figure 3). Most mAbs and plasma samples neutralized B.1.1.7 and mink cluster 5 variants at the same level as the prototypic 614G pseudovirus. B.1.1.7 was slightly resistant to mAbs 6-74 (3.3-fold) and 3-5 (6.0-fold) and was marginally resistant to plasma samples (1.0- to 2.9-fold change). The NTD-targeting mAb 6-74 was not effective against mink cluster 5, but 3-5 and most plasma samples had high potency against this variant. Neutralization resistance was observed for P.1 and especially B1.351 (Figures 3B and 3C). P.1 was not neutralized by mAbs 6-74 and 3-5 and required a high concentration of the other mAbs (2.6- to 8.0-fold) and plasma samples (1.4- to 4.0-fold). B.1.351 was neutralized by mAbs 9-105 and 10-121, but not by mAbs 6-74, 3-5, and 8-92. The potencies of 9-105 and 10-121 were reduced against B.1.351 (6.0- and 19-fold, respectively). B.1.351 was not neutralized by plasma samples from patient B or 202 DPSO from patient A (Figure 3B). Plasma samples at 36 and 57 DPSO from patient A neutralized B.1.351, although the potency decreased 5.5- and 3.2-fold compared with that against the prototypic virus, respectively.

All of the variants tested showed resistance to 6-74, suggesting that variants can easily escape from this mAb targeting the NTD, perhaps due to mutations in the NTD (Figure 3A). The efficacy of the RBD-targeting mAbs was decreased against P.1 and B.1.351, suggesting that the K417N/T, E484K, and N501Y mutations in the RBD region are critical for the resistance of these variants (Figure 3A). Analysis of single mutants revealed that K417N and K417T were critical for escape from 3-5 and slightly decreased the potency of 8-92 (Figure 3C, lower panels). E484K and N501Y single mutation did not confer resistance to

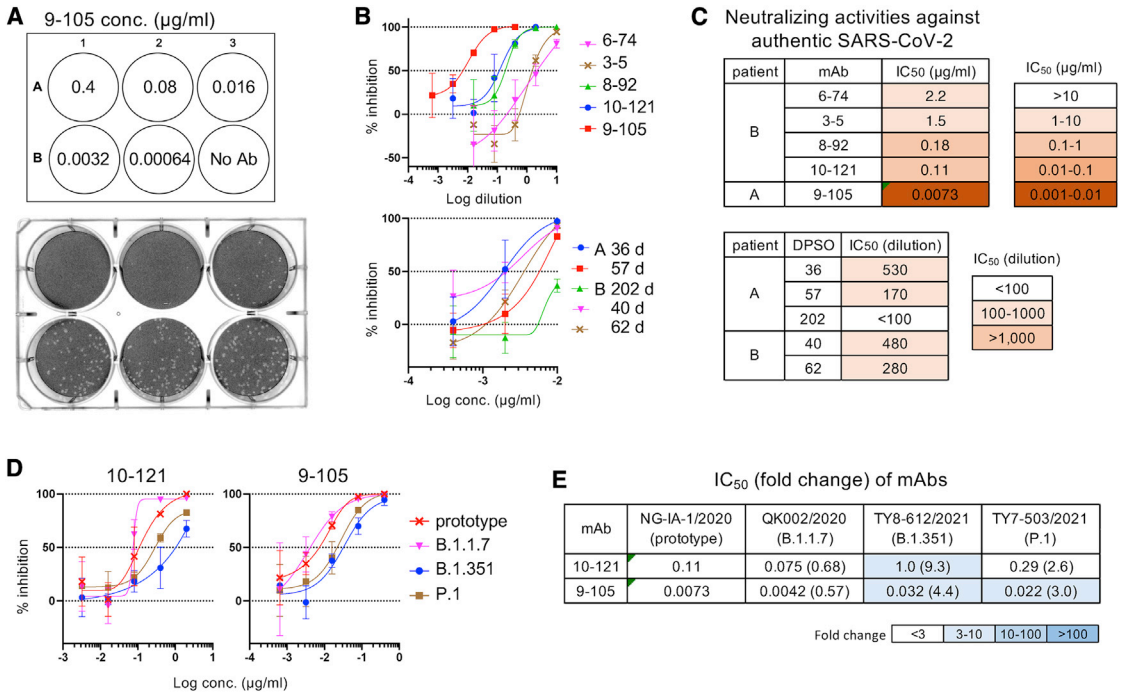

Figure 4. Neutralization of authentic SARS-CoV-2

(A) A plaque assay was performed using the authentic SARS-CoV-2 Japan/NGS-IA-1/2020 strain and Vero cells. Representative result of plaque formation in the presence of mAb 9-105 is shown.

(B) Neutralization of authentic SARS-CoV-2 by mAbs and plasma samples are shown.

(C) IC_{50} values of mAbs and plasma samples are summarized.

(D) Neutralization of authentic SARS-CoV-2 variants B.1.1.7, B.1.351, and P.1 by mAbs 10-121 and 9-105 are shown.

(E) IC_{50} values of mAbs (μg/mL) against authentic SARS-CoV-2 variants are summarized with fold change (variant IC_{50} value/prototype IC_{50} value).

Data shown in (B) and (D) are represented as means ± SD (n = 3). See also Figure S2 for structure of 9-105 and S complex.

these RBD-targeting mAbs. However, pseudoviruses with triple RBD mutations, especially the combination of K417N, E484K, and N501Y, were resistant to 3-5, 8-92, and 10-121. Interestingly, the potency of 9-105 was affected by K417N single mutation but neutralized triple mutants at the same level as prototype pseudovirus (Figure 3C, lower panels).

Neutralization resistance of P.1 and B.1.351 was observed in plasma samples from other patients with COVID-19, who were infected with SARS-CoV-2 before the spread of P.1 and B.1.351 in Japan (Figure 3D; Table S2). Analysis of plasma samples that had IC_{50} values greater than 1:100 against pseudovirus with SARS-CoV-2 S 614G revealed that neutralization sensitivity was maintained in the B.1.1.7 and mink cluster 5 variants but significantly decreased in the B.1.351 and P.1 variants. Only 2 of 14 plasma samples showed neutralizing activity against B.1.351, suggesting the high resistance of B.1.351 to neutralization by antibodies induced by prototypic SARS-CoV-2 infection (Figure 3D, upper right panel).

Neutralization of authentic SARS-CoV-2

The neutralizing activity of the five mAbs was also examined by infection of Vero cells with the authentic SARS-CoV-2 Japan/NGS-IA-1/2020 strain, which has an S protein identical to that of the Wuhan-Hu-1 strain. Consistent with the results using pseudovirus, 9-105 was the most potent mAb, and no plaque formation by infection was observed using 0.4 μg/mL 9-105 (Figure 4A). The neutralization activity of plasma samples and mAbs against authentic virus basically corresponded with those against pseudovirus (Figures 2A, 2C, 4B, and 4C).

The neutralization activity of the potent mAbs 10-121 and 9-105 was also examined against the authentic SARS-CoV-2 variants B.1.1.7 (Japan/QK002/2020), B.1.351 (Japan/TY8-612/2021), and P.1 (Japan/TY7-503/2021). Japan/QK002/2020 has the S protein identical to B.1.1.7 pseudovirus. Japan/TY8-612/2021 has the most S mutations of B.1.351 pseudovirus but lacks L18F and R246I. Japan/TY7-503/2021 has the same S mutations as P.1 pseudovirus and additionally has the V1176F mutation. Consistent with analysis using pseudoviruses, 9-105 and 10-121 neutralized these variants, although the potencies were reduced against B.1.351 and P.1 (Figures 4D and 4E).

DISCUSSION

The emergence of SARS-CoV-2 variants with multiple mutations in the S protein has raised concerns about the efficacy of antibodies elicited by infection or vaccination with prototypic SARS-CoV-2, which emerged in 2019. In this study, we examined the sensitivity of neutralizing mAbs and plasma samples

from two convalescent patients to emerging SARS-CoV-2 variants. Four of the five neutralizing mAbs isolated from these patients were RBD-targeting *VH3-53* antibodies, which are typically induced in patients with COVID-19 (Barnes et al., 2020; Brouwer et al., 2020; Cao et al., 2020; Gaebler et al., 2021; Kim et al., 2021; Kreye et al., 2020; Wu et al., 2020b). The most potent mAb, 9-105, neutralized SARS-CoV-2 pseudovirus with IC_{50} values ranging from 0.92 to 3.5 ng/mL in various target cells, indicating that 9-105 is one of the most potent mAbs against SARS-CoV-2 reported to date (Barnes et al., 2020; Brouwer et al., 2020; Cao et al., 2020; Kreye et al., 2020; Liu et al., 2020a).

Previous studies demonstrated that the sensitivity to plasma and mAbs isolated from convalescent patients or vaccinated individuals was moderately decreased against B.1.1.7 and markedly reduced against B.1.351 (Edara et al., 2021; Graham et al., 2021; Muik et al., 2021; Shen et al., 2021; Supasa et al., 2021; Tada et al., 2021; Wibmer et al., 2021; Wu et al., 2021). Consistent with these studies, our study showed a slight and severe decrease in the sensitivity of plasma and mAbs from convalescent patients against B.1.1.7 and B.1.351, respectively. Furthermore, we examined the sensitivity of other variants, P.1 and mink cluster 5, to antibodies. Mink cluster 5 was neutralized by plasma samples from convalescent patients at the same level as prototypic SARS-CoV-2, as reported previously (Tada et al., 2021; Wu et al., 2021). The neutralizing activity of mAbs was similar against prototypic and mink cluster 5 viruses, although 6-74, a mAb against the NTD region, did not neutralize mink cluster 5. In contrast, P.1 was resistant to most mAbs and some of the plasma samples. The resistance level of P.1 was between those of B.1.1.7 and B.1.351.

Variants were reported to be resistant to most NTD-targeting mAbs, including 6-74 examined in this study (Graham et al., 2021; McCallum et al., 2021; Wang et al., 2021). Mutations in the NTD, which are frequently observed in circulating variants, may occur as an escape from NTD-targeting neutralizing mAbs. On the other hand, mutations in the RBD of P.1 and B.1.351 marginally affected the potency of RBD-targeting mAbs when examined by point mutations, except for K417N/T, which resulted in escape from 3-5. The combination of three RBD mutations of P.1 and B.1.351 conferred a significant resistance to 8-92 and 10-121 but did not affect the potency of 9-105. Interestingly, 9-105 potency was slightly decreased by the K417N mutation but recovered to the same level as prototypic virus by the combination of three RBD mutations of P.1 and B.1.351 (Figure 3C). Resistance of B.1.351 to 9-105 may be responsible to the mutations outside the RBD.

The RBD-targeting mAbs tested in this study are typical *VH3-53* antibodies, which share structural similarities (Barnes et al., 2020; Cao et al., 2020; Kim et al., 2021; Wu et al., 2020b). Structural analysis suggests that 9-105 binds the RBD region overlapping the ACE2-binding site by interactions similar to other RBD-targeting *VH3-53* antibodies (Figure S2) (Barnes et al., 2020; Kaku et al., 2020; Wu et al., 2020b). The combination of RBD-targeting *VH3-53* mAbs in this study did not show any synergy in neutralizing activity (data not shown), suggesting that these mAbs recognize the overlapping region in the RBD. The strong binding affinity of 9-105 and 10-121 to RBD may be one reason for cross-neutralizing activity against B.1.351 and P.1 variants. The decrease in RBD binding affinity with mutations may be complemented by interacting with multiple sites of the RBD.

SARS-CoV-2 has evolved, and new variants continue to emerge. Adaptation to humans, such as the conformational change in the S protein by the D614G mutation (Gobeil et al., 2021; Weissman et al., 2021; Yurkovetskiy et al., 2020), may enhance its transmission in humans. Moreover, variants that mutate to escape from antibody neutralization, which occurs during chronic infection (Kemp et al., 2021; Starr et al., 2021), as well as selection by the prototypic SARS-CoV-2-based vaccine, are a major concern for the treatment and prevention of SARS-CoV-2. It is important to monitor the emergence of new variants and identify the mutations associated with immune escape.

STAR★METHODS

Detailed methods are provided in the online version of this paper and include the following:

- KEY RESOURCES TABLE
- RESOURCE AVAILABILITY
  - Lead contact
  - Materials availability
  - Data and code availability
- EXPERIMENTAL MODEL AND SUBJECT DETAILS
  - Sample collection from patients with COVID-19
  - Cell lines
- METHOD DETAILS
  - Isolation of IgG^+ memory B cells from patients with COVID-19
  - Cloning of immunoglobulin variable genes
  - Production and purification of recombinant IgG
  - Analysis of the binding activity of antibodies by flowcytometry
  - Analysis of the binding activity of mAbs by surface plasmon resonance
  - Analysis of the binding activity of mAbs to RBD and NTD
  - Neutralization assay using pseudovirus
  - DSP assay to monitor cell fusion
  - Neutralization of authentic virus
- QUANTIFICATION AND STATISTICAL ANALYSIS

SUPPLEMENTAL INFORMATION

Supplemental information can be found online at https://doi.org/10.1016/j.celrep.2021.109385.

ACKNOWLEDGMENTS

We thank all the clinical staff who provided care for the patients in Kumamoto City Hospital and Kyusyu Medical Center. We thank Dr. Misumi and Dr. Shuto (Kumamoto University) and Dr. Gohda (University of Tokyo) for providing cell lines, Dr. Yasuda (Nagasaki University) for providing authentic SARS-CoV-2, Dr. Ito (National Institute of Infectious Diseases) for providing authentic SARS-CoV-2 variants, and Dr. Tokunaga (National Institute of Infectious Diseases) for providing plasmids for pseudovirus production. We also thank Dr. Oshiumi (Kumamoto University) for cooperation in obtaining authentic SARS-CoV-2 variants and Dr. Croxford (Edanz Group) for editing a draft of

this manuscript. This study was supported by the Japan Agency for Medical Research and Development (grant JP20fk0108271 to S.M., T.K., Y. Maeda, and T.T; grant JP19fk0108111 to T.H.; and grant JP20fk0108270 to N.T. and Y. Koyanagi); a grant from the Senshin Medical Research Foundation to S.M.; Ministry of Education, Culture, Sports, Science and Technology KAKENHI grants 20H05773 and 20K20596 to T.H.; a grant from the JST Core Research for Evolutional Science and Technology (20356730) and the JSPS Core-to-Core Program A, the Advanced Research Networks to T.N. and Y. Koyanagi; an intramural grant from Kumamoto University COVID-19 Research Projects (AMABIE) to Y. Maeda, T.I., and C.M.; Kumamoto University International Collaborative Research Grants to T.U.; and the Joint Usage/Research Center program of the Institute for Frontier Life and Medical Sciences Kyoto University (S.M. and Y. Koyanagi).

AUTHOR CONTRIBUTIONS

Y. Kaku, T.K., and S.M. designed the experiments. H.I., Y.N., R.M., C.M, and M.T. collected patient samples. Y. Kaku isolated B cells. Y. Kaku., H.M.Z., N.K., S.B., K.M. M.S., Y.K., K.S., and C.O. performed antibody cloning. T.H., T.S., J.S., T.N, Y. Muramoto, Y. Kaku, and T.T produced proteins and performed binding assay. T.I., M.T., and T.K. prepared authentic viruses. T.K. performed neutralization assays. Y. Kaku, T.K., Y. Maeda, T.U., Y. Koyanagi, and S.M. interpreted data. Y. Kaku., T.K., and S.M. prepared the figures and wrote the paper. S.M. designed and coordinated the study.

DECLARATION OF INTERESTS

Y. Kaku, T.K., and S.M. are listed as inventors on a patent application related to this work. The remaining authors declare no competing interests.

Received: March 13, 2021
Revised: May 16, 2021
Accepted: June 18, 2021
Published: July 13, 2021

REFERENCES

Barnes, C.O., Jette, C.A., Abernathy, M.E., Dam, K.A., Esswein, S.R., Gristick, H.B., Malyutin, A.G., Sharaf, N.G., Huey-Tubman, K.E., Lee, Y.E., et al. (2020). SARS-CoV-2 neutralizing antibody structures inform therapeutic strategies. Nature *588*, 682–687.

Brochet, X., Lefranc, M.-P., and Giudicelli, V. (2008). IMGT/V-QUEST: the highly customized and integrated system for IG and TR standardized V-J and V-D-J sequence analysis. Nucleic Acids Res. *36*, W503-8.

Brouwer, P.J.M., Caniels, T.G., van der Straten, K., Snitselaar, J.L., Aldon, Y., Bangaru, S., Torres, J.L., Okba, N.M.A., Claireaux, M., Kerster, G., et al. (2020). Potent neutralizing antibodies from COVID-19 patients define multiple targets of vulnerability. Science *369*, 643–650.

Cao, Y., Su, B., Guo, X., Sun, W., Deng, Y., Bao, L., Zhu, Q., Zhang, X., Zheng, Y., Geng, C., et al. (2020). Potent Neutralizing Antibodies against SARS-CoV-2 Identified by High-Throughput Single-Cell Sequencing of Convalescent Patients' B Cells. Cell *182*, 73–84.e16.

Coronella, J.A., Telleman, P., Truong, T.D., Ylera, F., and Junghans, R.P. (2000). Amplification of IgG VH and VL (Fab) from single human plasma cells and B cells. Nucleic Acids Res. *28*, E85–E85.

Duan, K., Liu, B., Li, C., Zhang, H., Yu, T., Qu, J., Zhou, M., Chen, L., Meng, S., Hu, Y., et al. (2020). Effectiveness of convalescent plasma therapy in severe COVID-19 patients. Proc. Natl. Acad. Sci. USA *117*, 9490–9496.

Edara, V.V., Floyd, K., Lai, L., Gardner, M., Hudson, W., Piantadosi, A., Waggoner, J.J., Babiker, A., Ahmed, R., Xie, X., et al. (2021). Infection and mRNA-1273 vaccine antibodies neutralize SARS-CoV-2 UK variant. medRxiv, 2021.02.02.21250799.

Elbe, S., and Buckland-Merrett, G. (2017). Data, disease and diplomacy: GISAID's innovative contribution to global health. Glob. Chall. *1*, 33–46.

Fujino, T., Nomoto, H., Kutsuna, S., Ujiie, M., Suzuki, T., Sato, R., Fujimoto, T., Kuroda, M., Wakita, T., and Ohmagari, N. (2021). Novel SARS-CoV-2 Variant Identified in Travelers from Brazil to Japan. Emerg. Infect. Dis. J. *27*, 1243–1245.

Gaebler, C., Wang, Z., Lorenzi, J.C.C., Muecksch, F., Finkin, S., Tokuyama, M., Cho, A., Jankovic, M., Schaefer-Babajew, D., Oliveira, T.Y., et al. (2021). Evolution of antibody immunity to SARS-CoV-2. Nature *591*, 639–644.

Gobeil, S.M.C., Janowska, K., McDowell, S., Mansouri, K., Parks, R., Manne, K., Stalls, V., Kopp, M.F., Henderson, R., Edwards, R.J., et al. (2021). D614G Mutation Alters SARS-CoV-2 Spike Conformation and Enhances Protease Cleavage at the S1/S2 Junction. Cell Rep. *34*, 108630.

Graham, C., Seow, J., Huettner, I., Khan, H., Kouphou, N., Acors, S., Winstone, H., Pickering, S., Galao, R.P., Lista, M.J., et al. (2021). Impact of the B.1.1.7 variant on neutralizing monoclonal antibodies recognizing diverse epitopes on SARS-CoV-2 Spike. bioRxiv, 2021.02.03.429355.

He, L., Sok, D., Azadnia, P., Hsueh, J., Landais, E., Simek, M., Koff, W.C., Poignard, P., Burton, D.R., and Zhu, J. (2014). Toward a more accurate view of human B-cell repertoire by next-generation sequencing, unbiased repertoire capture and single-molecule barcoding. Sci. Rep. *4*, 6778.

Kaku, Y., Kuwata, T., Gorny, M.K., and Matsushita, S. (2020). Prediction of contact residues in anti-HIV neutralizing antibody by deep learning. Jpn. J. Infect. Dis. *73*, 235–241.

Kemp, S.A., Collier, D.A., Datir, R.P., Ferreira, I.A.T.M., Gayed, S., Jahun, A., Hosmillo, M., Rees-Spear, C., Mlcochova, P., Lumb, I.U., et al.; CITIID-NIHR BioResource COVID-19 Collaboration; COVID-19 Genomics UK (COG-UK) Consortium (2021). SARS-CoV-2 evolution during treatment of chronic infection. Nature *592*, 277–282.

Kim, S.I., Noh, J., Kim, S., Choi, Y., Yoo, D.K., Lee, Y., Lee, H., Jung, J., Kang, C.K., Song, K.H., et al. (2021). Stereotypic neutralizing V_H antibodies against SARS-CoV-2 spike protein receptor binding domain in patients with COVID-19 and healthy individuals. Sci. Transl. Med. *13*, eabd6990.

Kreye, J., Reincke, S.M., Kornau, H.C., Sánchez-Sendin, E., Corman, V.M., Liu, H., Yuan, M., Wu, N.C., Zhu, X., Lee, C.D., et al. (2020). A Therapeutic Non-self-reactive SARS-CoV-2 Antibody Protects from Lung Pathology in a COVID-19 Hamster Model. Cell *183*, 1058–1069.e19.

Kubota, M., Takeuchi, K., Watanabe, S., Ohno, S., Matsuoka, R., Kohda, D., Nakakita, S., Hiramatsu, H., Suzuki, Y., Nakayama, T., et al. (2016). Trisaccharide containing α2,3-linked sialic acid is a receptor for mumps virus. Proc. Natl. Acad. Sci. U S A *113*, 11579–11584.

Leung, K., Shum, M.H., Leung, G.M., Lam, T.T., and Wu, J.T. (2021). Early transmissibility assessment of the N501Y mutant strains of SARS-CoV-2 in the United Kingdom, October to November 2020. Euro Surveill. *26*, 2002106.

Li, L., Zhang, W., Hu, Y., Tong, X., Zheng, S., Yang, J., Kong, Y., Ren, L., Wei, Q., Mei, H., et al. (2020). Effect of Convalescent Plasma Therapy on Time to Clinical Improvement in Patients With Severe and Life-threatening COVID-19: A Randomized Clinical Trial. JAMA *324*, 460–470.

Liu, L., Wang, P., Nair, M.S., Yu, J., Rapp, M., Wang, Q., Luo, Y., Chan, J.F.W., Sahi, V., Figueroa, A., et al. (2020a). Potent neutralizing antibodies against multiple epitopes on SARS-CoV-2 spike. Nature *584*, 450–456.

Liu, S.T.H., Lin, H.-M., Baine, I., Wajnberg, A., Gumprecht, J.P., Rahman, F., Rodriguez, D., Tandon, P., Bassily-Marcus, A., Bander, J., et al. (2020b). Convalescent plasma treatment of severe COVID-19: a propensity score-matched control study. Nat. Med. *26*, 1708–1713.

Maggi, F., Novazzi, F., Genoni, A., Baj, A., Spezia, P.G., Focosi, D., Zago, C., Colombo, A., Cassani, G., Pasciuta, R., et al. (2021). Imported SARS-COV-2 Variant P.1 Detected in Traveler Returning from Brazil to Italy. Emerg. Infect. Dis. J. *27*, 1249–1251.

McCallum, M., De Marco, A., Lempp, F.A., Tortorici, M.A., Pinto, D., Walls, A.C., Beltramello, M., Chen, A., Liu, Z., Zatta, F., et al. (2021). N-terminal domain antigenic mapping reveals a site of vulnerability for SARS-CoV-2. Cell *184*, 2332–2347.e16.

Muik, A., Wallisch, A.-K., Sänger, B., Swanson, K.A., Mühl, J., Chen, W., Cai, H., Maurus, D., Sarkar, R., Türeci, Ö., et al. (2021). Neutralization of

SARS-CoV-2 lineage B.1.1.7 pseudovirus by BNT162b2 vaccine–elicited human sera. Science *371*, 1152–1153.

Ozono, S., Zhang, Y., Tobiume, M., Kishigami, S., and Tokunaga, K. (2020). Super-rapid quantitation of the production of HIV-1 harboring a luminescent peptide tag. J. Biol. Chem. *295*, 13023–13030.

Ozono, S., Zhang, Y., Ode, H., Sano, K., Tan, T.S., Imai, K., Miyoshi, K., Kishigami, S., Ueno, T., Iwatani, Y., et al. (2021). SARS-CoV-2 D614G spike mutation increases entry efficiency with enhanced ACE2-binding affinity. Nat. Commun. *12*, 848.

Rambaut, A., Holmes, E.C., O'Toole, Á., Hill, V., McCrone, J.T., Ruis, C., du Plessis, L., and Pybus, O.G. (2020). A dynamic nomenclature proposal for SARS-CoV-2 lineages to assist genomic epidemiology. Nat. Microbiol. *5*, 1403–1407.

Ramirez Valdez, K.P., Kuwata, T., Maruta, Y., Tanaka, K., Alam, M., Yoshimura, K., and Matsushita, S. (2015). Complementary and synergistic activities of anti-V3, CD4bs and CD4i antibodies derived from a single individual can cover a wide range of HIV-1 strains. Virology *475*, 187–203.

Sakurai, Y., Ngwe Tun, M.M., Kurosaki, Y., Sakura, T., Inaoka, D.K., Fujine, K., Kita, K., Morita, K., and Yasuda, J. (2021). 5-amino levulinic acid inhibits SARS-CoV-2 infection in vitro. Biochem. Biophys. Res. Commun. *545*, 203–207.

Schäfer, A., Muecksch, F., Lorenzi, J.C.C., Leist, S.R., Cipolla, M., Bournazos, S., Schmidt, F., Maison, R.M., Gazumyan, A., Martinez, D.R., et al. (2021). Antibody potency, effector function, and combinations in protection and therapy for SARS-CoV-2 infection in vivo. J. Exp. Med. *218*, 218.

Shen, X., Tang, H., McDanal, C., Wagh, K., Fischer, W., Theiler, J., Yoon, H., Li, D., Haynes, B.F., Sanders, K.O., et al. (2021). SARS-CoV-2 variant B.1.1.7 is susceptible to neutralizing antibodies elicited by ancestral spike vaccines. Cell Host Microbe *29*, 529–539.e3.

Soto, C., Finn, J.A., Willis, J.R., Day, S.B., Sinkovits, R.S., Jones, T., Schmitz, S., Meiler, J., Branchizio, A., and Crowe, J.E., Jr. (2020). PyIR: a scalable wrapper for processing billions of immunoglobulin and T cell receptor sequences using IgBLAST. BMC Bioinformatics *21*, 314.

Starr, T.N., Greaney, A.J., Addetia, A., Hannon, W.W., Choudhary, M.C., Dingens, A.S., Li, J.Z., and Bloom, J.D. (2021). Prospective mapping of viral mutations that escape antibodies used to treat COVID-19. Science *371*, 850–854.

Supasa, P., Zhou, D., Dejnirattisai, W., Liu, C., Mentzer, A.J., Ginn, H.M., Zhao, Y., Duyvesteyn, H.M.E., Nutalai, R., Tuekprakhon, A., et al. (2021). Reduced neutralization of SARS-CoV-2 B.1.1.7 variant by convalescent and vaccine sera. Cell *184*, 2201–2211.e7.

Tada, T., Dcosta, B.M., Samanovic-Golden, M., Herati, R.S., Cornelius, A., Mulligan, M.J., and Landau, N.R. (2021). Neutralization of viruses with European, South African, and United States SARS-CoV-2 variant spike proteins by convalescent sera and BNT162b2 mRNA vaccine-elicited antibodies. BioRxiv, 2021.02.05.430003.

Tegally, H., Wilkinson, E., Giovanetti, M., Iranzadeh, A., Fonseca, V., Giandhari, J., Doolabh, D., Pillay, S., San, E.J., Msomi, N., et al. (2021). Detection of a SARS-CoV-2 variant of concern in South Africa. Nature *592*, 438–443.

Tiller, T., Meffre, E., Yurasov, S., Tsuiji, M., Nussenzweig, M.C., and Wardemann, H. (2008). Efficient generation of monoclonal antibodies from single human B cells by single cell RT-PCR and expression vector cloning. J. Immunol. Methods *329*, 112–124.

Wang, P., Nair, M.S., Liu, L., Iketani, S., Luo, Y., Guo, Y., Wang, M., Yu, J., Zhang, B., Kwong, P.D., et al. (2021). Antibody resistance of SARS-CoV-2 variants B.1.351 and B.1.1.7. Nature *593*, 130–135.

Weinreich, D.M., Sivapalasingam, S., Norton, T., Ali, S., Gao, H., Bhore, R., Musser, B.J., Soo, Y., Rofail, D., Im, J., et al.; Trial Investigators (2021). REGN-COV2, a Neutralizing Antibody Cocktail, in Outpatients with Covid-19. N. Engl. J. Med. *384*, 238–251.

Weissman, D., Alameh, M.G., de Silva, T., Collini, P., Hornsby, H., Brown, R., LaBranche, C.C., Edwards, R.J., Sutherland, L., Santra, S., et al. (2021). D614G Spike Mutation Increases SARS CoV-2 Susceptibility to Neutralization. Cell Host Microbe *29*, 23–31.e4.

Wibmer, C.K., Ayres, F., Hermanus, T., Madzivhandila, M., Kgagudi, P., Oosthuysen, B., Lambson, B.E., de Oliveira, T., Vermeulen, M., van der Berg, K., et al. (2021). SARS-CoV-2 501Y.V2 escapes neutralization by South African COVID-19 donor plasma. Nat. Med. *27*, 622–625.

Wu, F., Zhao, S., Yu, B., Chen, Y.-M., Wang, W., Song, Z.-G., Hu, Y., Tao, Z.-W., Tian, J.-H., Pei, Y.-Y., et al. (2020a). A new coronavirus associated with human respiratory disease in China. Nature *579*, 265–269.

Wu, N.C., Yuan, M., Liu, H., Lee, C.D., Zhu, X., Bangaru, S., Torres, J.L., Caniels, T.G., Brouwer, P.J.M., van Gils, M.J., et al. (2020b). An Alternative Binding Mode of IGHV3-53 Antibodies to the SARS-CoV-2 Receptor Binding Domain. Cell Rep. *33*, 108274.

Wu, K., Werner, A.P., Moliva, J.I., Koch, M., Choi, A., Stewart-Jones, G.B.E., Bennett, H., Boyoglu-Barnum, S., Shi, W., Graham, B.S., et al. (2021). mRNA-1273 vaccine induces neutralizing antibodies against spike mutants from global SARS-CoV-2 variants. BioRxiv, 2021.01.25.427948.

Yamamoto, M., Kiso, M., Sakai-Tagawa, Y., Iwatsuki-Horimoto, K., Imai, M., Takeda, M., Kinoshita, N., Ohmagari, N., Gohda, J., Semba, K., et al. (2020). The Anticoagulant Nafamostat Potently Inhibits SARS-CoV-2 S Protein-Mediated Fusion in a Cell Fusion Assay System and Viral Infection In Vitro in a Cell-Type-Dependent Manner. Viruses *12*, 629.

Yurkovetskiy, L., Wang, X., Pascal, K.E., Tomkins-Tinch, C., Nyalile, T.P., Wang, Y., Baum, A., Diehl, W.E., Dauphin, A., Carbone, C., et al. (2020). Structural and Functional Analysis of the D614G SARS-CoV-2 Spike Protein Variant. Cell *183*, 739–751.e8.

Zhou, P., Yang, X.-L., Wang, X.-G., Hu, B., Zhang, L., Zhang, W., Si, H.-R., Zhu, Y., Li, B., Huang, C.-L., et al. (2020). A pneumonia outbreak associated with a new coronavirus of probable bat origin. Nature *579*, 270–273.

Zhu, N., Zhang, D., Wang, W., Li, X., Yang, B., Song, J., Zhao, X., Huang, B., Shi, W., Lu, R., et al.; China Novel Coronavirus Investigating and Research Team (2020). A Novel Coronavirus from Patients with Pneumonia in China, 2019. N. Engl. J. Med. *382*, 727–733.

STAR★METHODS

KEY RESOURCES TABLE

REAGENT or RESOURCE	SOURCE	IDENTIFIER
Antibodies		
Biotin CD3 Monoclonal Antibody (UCHT1)	eBioscience	Cat#13-0038-82, RRID:AB_466323
Biotin Mouse Anti-Human CD8 (RPA-T8)	BD	Cat#555365; RRID:AB_395768
Biotin CD14 Monoclonal Antibody (61D3)	eBioscience	Cat#13-0149-82; RRID:AB_466373
Anti-human CD19 Antibody FITC (HIB19)	BioLegend	Cat#302206; RRID:AB_314236
Anti-human IgM Antibody APC/Cy7 (MHM-88)	BioLegend	Cat#314520; RRID:AB_10900422
Anti-Human IgG BV421 (G18-145)	BD	Cat#562581; RRID:AB_2737665
anti-human CD27 Antibody PE (M-T271)	BioLegend	Cat#356406; RRID:AB_2561825
APC-conjugated AffiniPure F(ab')2 Fragment Goat Anti-Human IgG (H + L)	Jackson ImmunoResearch	Cat#109-136-088; RRID:AB_2337691
Bacterial and virus strains		
SARS-CoV-2 Japan/NGS-IA-1/2020	Sakurai et al., 2021	GISAID ID number: EPI_ISL_481251
SARS-CoV-2 Japan/TY7-503/2021	National Institute of Infectious Diseases, Japan	GISAID ID number: EPI_ISL_877769
SARS-CoV-2 Japan/TY8-612-P1/2021	National Institute of Infectious Diseases, Japan	GISAID ID number: EPI_ISL_1123289
SARS-CoV-2 Japan/QK002/2020	National Institute of Infectious Diseases, Japan	GISAID ID number: EPI_ISL_768526
Stbl2 Competent Cells	Invitrogen	Cat#10268019
Biological samples		
Blood of SARS-CoV-2 infected patient A and B, See Table S1	This paper	N/A
Plasma of SARS-CoV-2 infected individuals, See Table S2	This paper	N/A
Chemicals, peptides, and recombinant proteins		
MojoSort Magnet	BioLegend	Cat#480019
7AAD	BD	Cat#559925
guanidine thiocyanate	Invitrogen	Cat#AM9422
dNTP-Mix (10mM)	Invitrogen	Cat#18427088
Recombinant RNase inhibitor	Takara	Cat#2313B
Superscript III reverse transcriptase	Invitrogen	Cat#18080085
Sensor Chip CM5	cytiva	Cat#BR100030
Human Antibody Capture Kit	cytiva	Cat#BR100839
Amine Coupling Kit	cytiva	Cat#BR100050
G418	Millipore	Cat#345812-20ML
Hygromycin B	Nacalai Tesque	Cat#09287-84
RBD	This paper	N/A
NTD	This paper	N/A
Protein A AlphaScreen Donor Beads	PerkinElmer	Cat#AS102D
Anti-His AlphaLISA Acceptor beads	PerkinElmer	Cat#AL178C
Carboxymethyl cellulose	Sigma	Cat#C9481-500G
Methylene blue	Nacalai Tesque	Cat#22412-14

(*Continued on next page*)

Continued

REAGENT or RESOURCE	SOURCE	IDENTIFIER
Critical commercial assays		
FectoPRO	Polyplus-transfection	Cat#116-010
FectoCHO Expression System	Polyplus-transfection	Cat#716-06LKIT
Luciferase assay system	Promega	Cat#E4550
EnduRen	Promega	Cat#E6481
Gibson Assembly Master Mix	New England Biolabs	Cat#E2611L
HiTrap rProtein A FF Column	cytiva	Cat#17507901
COSMOGEL His-Accept	Nacalai Tesque	Cat#09277-56
Superdex 75 Increase 10/300 GL	cytiva	Cat#29148721
Deposited data		
Antibody nucleotide sequence	This paper	GenBank accession number: MZ089617 to MZ089626
Structure of antibody (COVA2-04 or COVA2-39)-RBD complex	Wu et al., 2020b	PDB: 7JMO and 7JMP
Structure of 9-105-RBD complex	This paper	N/A
Experimental models: cell lines		
293T	ATCC	CRL-3216
293A	Invitrogen	Cat#R70507
293FT/DSP1-7/ACE2/TMPRSS2	Yamamoto et al., 2020	N/A
293FT/DSP8-11/SARS-CoV-2-S	Yamamoto et al., 2020	N/A
Calu3-DSP1-7	Yamamoto et al., 2020	N/A
Calu-3	ATCC	HTB-55
Caco-2	ATCC	HTB-37
Vero	ATCC	CCL-81
ExpiCHO-S	GIBCO	Cat#A29127
Oligonucleotides		
Primer: 3′ Cγ CH1: GGAAGGTGTGCACGCCGCTGGTC	Tiller et al., 2008	N/A
Primer: HcnestU: GG(ACTAGT)TCTTGTCCACCTTGGTGTTG	Coronella et al., 2000	N/A
Primer: P1-Cκ (modified): CAGCAGGCACACAACAGAGGCAGTTCC	He et al., 2014	N/A
Primer: 3′ Cλ: CACCAGTGTGGCCTTGTTGGCTTG	Tiller et al., 2008	N/A
Primer: Lnest: GCTCTAGAACTAATGCGTGACCTGGCAGCTGT	Coronella et al., 2000	N/A
Recombinant DNA		
pIgGH	Ramirez Valdez et al., 2015	N/A
pKVA2	Ramirez Valdez et al., 2015	N/A
pLSH	Ramirez Valdez et al., 2015	N/A
SARS-CoV-2 Spike ORF expression plasmid	Sino Biological	Cat#VG40589-UT
pSARS-CoV-2-S-IRES-EGFP	This paper	N/A
psPAX2-IN/HiBiT	Ozono et al., 2020	N/A
pWPI-Luc2	Ozono et al., 2020	N/A
pC-SARS2-S-D614G	Ozono et al., 2021	N/A
pSARS-CoV-2-S-D614G-19del	This paper	N/A
SARS-CoV S-expressing plasmid	Sino Biological	Cat#VG40150-G-N
MERS-CoV S-expressing plasmid	Sino Biological	Cat#VG40069-G-N
Plasmids to express pSARS-CoV-2 S variants	This paper	N/A
Plasmids to express pSARS-CoV-2 S mutants	This paper	N/A

(*Continued on next page*)

Continued

REAGENT or RESOURCE	SOURCE	IDENTIFIER
Software and algorithms		
IMGT vquest	Brochet et al., 2008	http://imgt.org/
PyIR	Soto et al., 2020	https://github.com/crowelab/PyIR
FlowJo	TreeStar	Version 10.7.1 https://www.flowjo.com
BIAevaluation	GE healthcare	Version 4.1 http://www.cytivalifesciences.com/country-selection?originalItemPath=%2f
Prism	GraphPad Software	Version 8.4.3 https://www.graphpad.com/scientific-software/prism/

RESOURCE AVAILABILITY

Lead contact

Further information and requests for resources and reagents should be directed to and will be fulfilled by the Lead Contact, Shuzo Matsushita (shuzo@kumamoto-u.ac.jp).

Materials availability

Further information and requests for resources and reagents should be directed to Shuzo Matsushita (shuzo@kumamoto-u.ac.jp).

Data and code availability

- Sequence data for antibodies have been deposited at GenBank and are publicly available as of the date of publication. Accession numbers are listed in the key resources table.
- This paper does not report original code.
- Any additional information required to reanalyze the data reported in this paper is available from the lead contact upon request.

EXPERIMENTAL MODEL AND SUBJECT DETAILS

Sample collection from patients with COVID-19

Peripheral blood samples were obtained from donors hospitalized in Kumamoto City Hospital and Kyushu Medical Center, who recovered from COVID-19 disease. Peripheral blood samples for antibody isolation were obtained from patients A (male) and B (male), and the information of patients were in Table S1. Age of these patients are undisclosed due to privacy policy. Information of patients with COVID-19 other than patients A and B is in Table S2. The study protocol was approved by the institutional ethical review boards of Kumamoto City Hospital (546), Kyushu Medical Center (20C120) and Kumamoto University (2013 and 2066). All the study participants provided their written informed consent for the collection of the samples and their subsequent analysis. All the patient samples were collected before the emergence of variants tested in this study.

Cell lines

Human embryonic kidney cells, 293T, 293A, 293FT/DSP1-7/ACE2/TMPRSS2 and 293FT/DSP8-11/SARS-CoV2-S, were maintained in high glucose DMEM (Nacalai Tesque) supplemented with 10% fetal bovine serum (FBS, Sigma-Aldrich). Calu-3 (human lung cancer cell line), Calu-3-DSP1-7 and Caco-2 (human colon adenocarcinoma cell line) cells were maintained in EMEM with non-essential amino acids (Fujifilm) supplemented with 20% FBS. Vero cells were maintained in EMEM (Fujifilm) supplemented with 5% FBS. ExpiCHO-S cells were maintained in ExpiCHO Expression Medium (Invitrogen).

METHOD DETAILS

Isolation of IgG^+ memory B cells from patients with COVID-19

Samples collected from patient A 36 and 57 DPSO and patient B 40 DPSO were used for isolation of mAbs. Peripheral blood mononuclear cells were isolated by Ficoll density gradient centrifugation and B cells were enriched by negative selection using antibodies against CD3 CD8 and CD14 nd MojoSort Magnet. The enriched B cells were stained with 7AAD, CD19-FITC, IgM-APC/Cy7, IgG-BV421 and CD27-PE. IgG^+ memory B cells ($7AAD^-CD19^+IgM^-IgG^+CD27^+$ cells) were sorted at single cell density into 5 μl/well of 50 μM ice-cold guanidine thiocyanate.

Cloning of immunoglobulin variable genes

Reverse transcription was performed in a total volume of 20 μl/well in a 96-well sorting plate containing 1.4 μL of 100 μM gene specific primers (Coronella et al., 2000; He et al., 2014; Tiller et al., 2008), 2 μL of 10 mM each dNTP-Mix, 1 μL of 0.1 M DTT, 20 U recombinant

RNase inhibitor, 4 μL of 5X First-Strand Buffer and 50 U Superscript III reverse transcriptase as follows: 42°C for 10 min, 25°C for 10 min, 50°C for 60 min and 94°C for 5 min.

Nested PCR was performed for cloning of immunoglobulin variable genes, as previously described (Ramirez Valdez et al., 2015). IgG heavy and light chain expression plasmids were constructed by the homologous recombination of the nested PCR products with pIgGH, pKVA2 and pLSH, respectively using the Gibson Assembly Master Mix. The nucleotide sequences of the immunoglobulin variable regions were analyzed for germline gene verification, framework and CDR mapping and quantification of percent identity to germline using IMGT vquest (Brochet et al., 2008) and PyIR, which is an IgBLAST wrapper and parser (Soto et al., 2020).

Production and purification of recombinant IgG

Recombinant IgG was produced and purified as previously described (Ramirez Valdez et al., 2015). Briefly, a pair of heavy and light chain plasmids were transfected into 293T cells using FectoPRO and the supernatant 2 days post transfection was used for the screening of antibodies reactive to SARS-CoV-2 S. Many antibodies were produced by the transient transfection of ExpiCHO cells with the FectoCHO Expression Kit or the establishment of 293A cells stably expressing IgG, which were cloned from colonies selected with G418 (1000 μg/ml) and hygromycin (150 μg/ml) from the cells transfected with heavy and light chain plasmids. IgG were purified using a HiTrap rProtein A FF Column.

Analysis of the binding activity of antibodies by flowcytometry

The binding activity of antibodies was analyzed using cells expressing SARS-CoV-2 S and enhanced green fluorescent protein (EGFP). The internal ribosome entry site (IRES) and the EGFP gene were inserted into a SARS-CoV-2 Spike ORF mammalian expression plasmid, and the resultant plasmid, pSARS-CoV-2-S-IRES-EGFP, was used for the transfection of 293T and 293A cells. Transiently or stably transfected cells were stained with primary antibody for 15 min at room temperature (RT). The cells were washed twice with PBS containing 0.2% BSA and incubated with APC-conjugated AffiniPure F(ab')2 Fragment Goat Anti-Human IgG (H + L) for 15 min at RT. The stained cells were analyzed by FACSCanto II (BD Biosciences). The reactivity of antibodies was analyzed after gating on EGFP+ cells using FlowJo.

Analysis of the binding activity of mAbs by surface plasmon resonance

Surface plasmon resonance (SPR) experiments were performed using a Biacore 3000 system (cytiva). For the mAb 9-105, anti-human IgG antibody was immobilized on a CM5 sensor chip by amine-coupling using a human Antibody capture kit, and then the mAb was immobilized on an anti-human IgG antibody-coupled chip. The RBD-9-105 complex was removed for regeneration because the bound RBD was not released from 9-105 under conventional regeneration conditions. Other mAbs were immobilized on the CM5 sensor chip by amine-coupling using an amine-coupling kit. Purified RBD (2–2500 nM) in HBS-P buffer (10 mM HEPES, 150 mM NaCl, 0.005% surfactant P20, pH 7.4) was injected over the immobilized mAbs. The binding response at each concentration was calculated by subtracting the equilibrium response measured in the control flow cell from the response in each sample flow cell. The data were analyzed using BIAevaluation version 4.1 software and K_d values were determined by equilibrium analyses using nonlinear curve fitting of the Langmuir binding isotherm.

Analysis of the binding activity of mAbs to RBD and NTD

Protein expression and purification of the S-protein RBD (amino acid number, P322 to N536) and NTD (amino acid number, S12 to S305) were performed as previously described for other viral glycoproteins (Kubota et al., 2016). Briefly, an expression plasmid encoding RBD or NTD was transiently transfected into 80% confluent HEK293 cells. At 6 days post-transfection, supernatant containing the secreted protein was harvested. Then, RBD or NTD was purified using COSMOGEL His-Accept in purification buffer (50 mM NaH_2PO_4, 150 mM NaCl, 10 mM imidazole, pH 8.0), and eluted with elution buffer (50 mM NaH_2PO_4, 150 mM NaCl, 500 mM imidazole, pH 8.0). RBD or NTD was further purified using a gel filtration column Superdex 75 Increase 10/300 GL in buffer containing 100 mM NaCl and 20 mM Tris-HCl (pH 8.0).

An AlphaScreen assay was performed as described in the manufacturer's protocol (PerkinElmer). In brief, 5 μL of recombinant IgG and supernatant from the transfected cells, were mixed with 50 ng of RBD or NTD. After incubation at 37°C for 40 min, 12.5 μg of Protein A AlphaScreen Donor Beads and Anti-6xHis AlphaLISA Acceptor beads were added to the reaction mix, respectively. After incubation at 37°C for 40 min, the AlphaScreen score was measured by EnSpire Multimode Plate Reader (PerkinElmer).

Neutralization assay using pseudovirus

The neutralization activity of antibodies was determined using HIV-1-based pseudovirus with SARS-CoV-2 S, as previously described (Ozono et al., 2020, 2021) In brief, 293T cells were transfected with lentiviral packaging plasmid psPAX2-IN/HiBiT, the firefly luciferase-expressing lentiviral transfer plasmid pWPI-Luc2 and a plasmid expressing SARS-CoV-2 S. We used pSARS-CoV-2-S-D614G-19del expressing S with the D614G mutation and a 19 amino acid deletion in the cytoplasmic tail, which was constructed from an S-expressing plasmid and pC-SARS2-S-D614G (Ozono et al., 2021), as a prototypic S. Plasmids to express S of variants and mutants were constructed by PCR-mutagenesis from pSARS-CoV-2-S-D614G-19del. Supernatant after 48 h of transfection was stored at −80°C. The median tissue culture infectious dose ($TCID_{50}$) of each pseudovirus was determined by infection with serially-diluted viruses. The neutralization assay was performed in triplicate. Serially diluted antibody and virus (200 $TCID_{50}$) were

incubated for 1 h and transferred to cells plated at 1-2x10^4 cells/well in a 96-well plate 1 day before infection. After incubation for 2 h, medium was changed to fresh medium, and incubated for an additional 48 h. Luciferase activity was measured using luciferase assay system and EnSpire Multimode Plate Reader (PerkinElmer). The relative light units (RLU) were compared to calculate the reduction in infectivity and 50% of the maximal inhibitory concentration (IC_{50}) was calculated using Prism 8.

DSP assay to monitor cell fusion

Cell fusion was analyzed using 293FT/DSP1-7/ACE2/TMPRSS2, 293FT/DSP8-11/SARS-CoV-2-S and Calu-3/DSP1-7 cells, as previously described (Yamamoto et al., 2020). Briefly, 293FT/DSP1-7/ACE2/TMPRSS2 and Calu-3/DSP1-7 cells, which were seeded in a 6-well plates (9 × 10^5 cells/3 ml) one day before the assay, were treated with 6 μM EnduRen. Serially-diluted mAb or plasma were added to a96-well black plate, in which 293FT/DSP8-11/SARS-CoV-2-S cells (3x10^4 cells/100 μl) were seeded one day before. After 2-4 h of EnduRen incubation, cells were detached and the 50 μl cell suspension was transferred to a 96-well black plate. Luciferase activity was measured periodically using EnSpire Multimode Plate Reader. The RLU were compared to calculate the reduction in infectivity and IC_{50} was calculated using Prism 8. Results of cell fusion using 293FT/DSP1-7/ACE2/TMPRSS2 and Calu-3/DSP1-7 cells at 6 h and 20 h after coculture, respectively, are shown.

Neutralization of authentic virus

Plaque assays were performed using Japan/NGS/IA-1/2020 (Sakurai et al., 2021), Japan/TY7-503/2021, Japan/TY8-612-P1/2021, and Japan/QK002/2020 strains of SARS-CoV-2. Vero cells were plated at 5x10^5 cells/well in a 6-well plate or 2x10^5 cells/well in a 12-well plate 1 day before experiment. Plasma or mAb was serially diluted in virus dilution buffer containing 1x MEM, 20 mM HEPES, 1x NEAA, and 1x penicillin and streptomycin. The diluted mAb or plasma (110 μl) was added to the same volume as 110 PFU of SARS-CoV-2, and incubated for 1 h. In 6-well plate, 50μl or 150 μl of the mixture was added to Vero cells supplemented with 950 μl or 850 μl of dilution buffer, respectively. In 12-well plate, 40μl or 160 μl of the mixture was added to Vero cells supplemented with 460 μl or 340 μl of dilution buffer, respectively. After incubation for 2 h, 2 and 1 mL PFU buffer containing 1x MEM, 3% FBS, and 1.5% carboxymethyl cellulose was overlaid to 6-well plate and 12-well plate, respectively. After further incubation for 3 days, wells were washed three times with PBS, and cells were fixed with 4% paraformaldehyde in PBS. Wells were washed with water, dried, and stained with 0.1% methylene blue to visualize the plaques. IC_{50} values were calculated using Prism 8.

QUANTIFICATION AND STATISTICAL ANALYSIS

Neutralization and fusion inhibition data are processed by Prism 8, and shown by the means ± SD of triplicates. The statistical analysis for comparison of IC_{50} values were performed using Prism 8 by Wilcoxon matched-pairs signed rank test where $p < 0.05$ are considered significant.